Published in final edited form as:
Arthritis Rheum. 2012 March ; 64(3): 895–907. doi:10.1002/art.33368.

Mutations in *PSMB8* Cause CANDLE Syndrome with Evidence of Genetic and Phenotypic Heterogeneity

Yin Liu, MD[1,*], **Yuval Ramot, MD, MSc**[2,3,*], **Antonio Torrelo, MD**[4], **Amy S. Paller, MD, MS**[5], **Nuo Si, BM**[6], **Sofia Babay, BSc**[3], **Peter W. Kim, MD**[7], **Afzal Sheikh**[7], **Chyi-Chia Richard Lee, MD, PhD**[8], **Yongqing Chen, MD, PhD**[1], **Angel Vera, MD**[9], **Xue Zhang, MD, PhD**[6], **Raphaela Goldbach-Mansky, MD, MHS**[1,*], and **Abraham Zlotogorski, MD**[2,3,*]

[1]National Institute of Arthritis and Musculoskeletal and Skin Diseases, National Institutes of Health Bethesda, MD, USA

[2]Department of Dermatology, Hadassah-Hebrew University Medical Center, Jerusalem, Israel

[3]Center for Genetic Diseases of the Skin and Hair, Hadassah-Hebrew University Medical Center, Jerusalem, Israel

[4]Departments of Pediatric Dermatology, Hospital Niño Jesús, Madrid

[5]Departments of Dermatology and Pediatrics, Feinberg School of Medicine, Northwestern University, Chicago, IL, USA

[6]McKusick-Zhang Center for Genetic Medicine and State Key Laboratory of Medical Molecular Biology, Institute of Basic Medical Sciences, Chinese Academy of Medical Sciences & Peking Union Medical College, Beijing, China

[7]National Human Genome Research Institute, National Institutes of Health Bethesda, MD, USA

[8]National Cancer Institute, National Institutes of Health Bethesda, MD, USA

[9]Hospital Carlos Haya, Málaga, Spain

Abstract

Objective—Chronic atypical neutrophilic dermatosis with lipodystrophy and elevated temperature (CANDLE) syndrome is an autoinflammatory syndrome recently described in children. We investigated the clinical phenotype, genetic cause and the immune dysregulation in nine CANDLE patients.

Methods—Genomic DNA from all patients was screened for *PSMB8* (Proteasome subunit beta type-8) mutations. Serum cytokine levels were measured from four patients. Skin biopsies were evaluated immunohistochemically and blood microarray profile (n=4) and stat-1 phosphorylation (n=3) were assessed.

Results—One patient was homozygous for a novel nonsense mutation in *PSMB8* (c.405C>A) suggesting a protein truncation, four patients were homozygous and two were heterozygous for a previously reported missense mutation (c.224C>T), and one patient showed no mutation. None of these sequence changes was observed in chromosomes from 750 healthy controls. Of the four patients with the same mutation, only two share the same haplotype indicating a mutational hot

Address correspondence to: Abraham Zlotogorski, MD, Department of Dermatology, Hadassah-Hebrew University Medical Center, Jerusalem 91120, Israel, zloto@cc.huji.ac.il, Phone: +972-507874158 or Raphaela Goldbach-Mansky, MD, MHS, NIAMS, NIH, Bethesda, MD 20892, USA, goldbacr@mail.nih.gov, Phone: +301-435-6243.
*These authors contributed equally to this work

Conflict of interest: None.

spot. *PSMB8* mutation-positive and -negative patients expressed high IP-10 (Interferon gamma-induced protein 10) levels. Levels of MCP-1, IL-6, and IL-1Ra were moderately elevated. Microarray profiles and monocyte stat-1 activation suggested a unique interferon (IFN) signaling signature, unlike in other autoinflammatory disorders.

Conclusion—CANDLE is caused by mutations *in PSMB8,* a gene recently reported to cause JMP syndrome (joint contractures, muscle atrophy and panniculitis induced lipodystrophy) in adults. We extend the clinical and pathogenic description of this novel autoinflammatory syndrome, thereby expanding the clinical and genetic disease spectrum of *PSMB8*-associated disorders. IFN may be a key mediator of the inflammatory response and may present a therapeutic target.

Auto-inflammatory diseases were first characterized more than 10 years ago by episodic, systemic and organ-specific inflammation (1, 2). These disorders differ from autoimmune diseases in that they primarily result from perturbations in the innate immune system, rather than in adaptive immunity, although overlapping features may occur (2, 3). During the past decade, the genetic basis for many autoinflammatory diseases has been revealed (1). Elucidating the underlying molecular basis for these monogenic disorders has increased the understanding of inflammation and has led to improved therapy, particularly interleukin-1 (IL-1) inhibition for patients with cryopyrin-associated periodic syndromes (CAPS) (4).

Chronic atypical neutrophilic dermatosis with lipodystrophy and elevated temperature (CANDLE syndrome) is a newly described autoinflammatory condition, now reported in five patients (5, 6). It is characterized by onset during the first year of life, recurrent fevers, purpuric skin lesions, violaceous swollen eyelids, arthralgias, progressive lipodystrophy, hypochromic or normocytic anemia, delayed physical development and increased acute phase reactants. Variable clinical features include hypertrichosis, acanthosis nigricans and alopecia areata (5, 6). The skin biopsy findings of a characteristic atypical, mixed mononuclear and neutrophilic infiltrate further confirm the diagnosis (5). A genetic etiology was suggested, possibly inherited in an autosomal recessive pattern. In order to elucidate the molecular basis of CANDLE syndrome, we performed genome-wide analysis and sequencing in eight families with nine affected patients.

MATERIALS AND METHODS

Patients

The present study includes nine patients (3 Spanish, 3 Hispanic, 1 Ashkenazi Jew and 2 American/Caucasian) from eight families who were seen at five international centers (two in Spain, Israel and two in the US). The study was approved by the institutional review board at the respective sites and written informed consent was obtained from the subjects or their parents. Blood samples were collected from eight patients and their unaffected family members where available. All of the patients included in this study were discussed among the lead investigators of the five centers to ensure the diagnosis of CANDLE before they were included. All patients had to have episodic fevers, typical erythematous eruptions, arthralgia/arthritis and evidence of systemic inflammation (elevation of acute phase reactants). In addition, a skin biopsy showing an atypical mixed myeloid, neutrophilic, and histiocytic infiltrate positive for myeloperoxidase and CD68 had to be present. Patients 1–4 were previously described by Torrelo et al. (5), and patient 5 was reported by Ramot et al. (6); patient 3 died at 14 years of age, and blood samples were not available for analysis (5). Patients 6–9 have not been described before.

Genetic Analysis

A genome-wide analysis of single-nucleotide polymorphisms was performed using the GeneChip Human Mapping 250K SNP Array of Affymetrix. For this analysis we used the blood samples of patients 1, 2, 4, 5 and 9. Genome-wide homozygosity analysis was performed by Homozygosity Mapper (7).

In parallel with the conventional Sanger sequencing, we also performed whole exome sequencing in patient 5. DNA captured with the Agilent SureSelect Human All Exon 50Mb kit was sequenced on an Illumina HiSeq 2000 platform. Sequence data were analyzed with a custom bioinformatics pipeline.

To identify additional mutations in *PSMB8* (Proteasome subunit beta type-8) in the two patients who are heterozygous for the *PSMB8* mutation T75M, and in the patient who did not have any mutation in *PSMB8* on exonic sequencing, we sequenced the other five exons and all of the introns of the longest isoform of *PSMB8* (Ensemble nomenclature, PSMB8.001). Alternative and cryptic splicing events were ruled out by sequencing the cDNA. We searched for genomic deletions by long range PCR with primers spanning the entire gene and ruled out the possibility of a heterozygous deletion at the primer binding site by sequencing the c.224C>T mutation using the long range PCR amplicon as template. In patients 6 and 7 both the maternal and paternal copies are present at *PSMB8* locus, and the *PSMB8* cDNA is of full-length (8). Assuming digenic inheritance in patient 7, we sequenced all the other beta subunits from *PSMB1* to *PSMB10* and two alpha subunits (*PSMA6* and *PSMA7*). *PSMB8* mRNA levels are similar to healthy controls by RT-qPCR from cDNA made from peripheral blood.

In silico modeling

A structural model of both mutations identified was assembled. Structures are based on a previously published model (9). Figures were made with Pymol.

Cytokine Analysis

Serum was collected from patients 6, 7 and 8 and stored at −80°C. Cytokine concentrations were measured using the Bio-Plex system (Bio-Rad) in batches including patient control and healthy serum.

Microarray analysis

Total RNA was extracted from blood samples collected in Paxgene tubes (from patients 4, 6, 7, and 8) and processed as recommended by the manufacturer (Qiagen). RNA integrity was analyzed with an Agilent 2100 Bioanalyzer. cDNA synthesis and target amplification was done with the NuGene Ovation® Whole Blood Solution kit. Affimetrix HU-133 plus 2.0 gene chips were used for hybridization. Data analysis was done with Genespring 11.5 software and Partek software, after removal of non-annotated genes. Genes differentially expressed in comparison to the mean expression in healthy controls were at least 2 fold higher (FCH>2) with a p-value less than 0.05 adjusted for multiple hypotheses testing and controlling the false-discovery rate (FDR) (FDR<0.05). Groups were compared using the two-tailed Welch t-test. DEGs were then analyzed in Ingenuity pathway analysis (IPA) (Ingenuity Systems, Inc., http://www.ingenuity.com) to investigate dysregulated canonical pathways and gene ontology. Results for interferon induced genes were plotted as a heat map with upregulated genes in shades of red and downregulated genes in shades of blue.

Cell stimulation and Stat-1 phosphorylation assay

Peripheral blood mononuclear cells (PBMC) were isolated by standard Ficoll density gradient centrifugation and frozen in liquid nitrogen. Cells were thawed, washed and resuspended in 0.1% BSA PBS at 2×10^6/ml and then aliquoted at 0.5ml per tube. For studies with the small molecule JAK kinase inhibitor tofacitinib[3-[(3*R*,4*R*)-4-methyl-3-[methyl(7*H*-pyrrolo[2,3-d]pyrimidin-4-yl)amino]piperidin-1-yl]-3-oxopropanenitrile, synthesized by Dr. Craig Thomas, NCGC/NIH], cells were treated with the inhibitor for 15 min before stimulation. Cells were stimulated with various concentrations of IFN-γ or control PBS buffer at 37°C for 15 min, fixed with 4% paraformaldehyde and then stained with CD14.PE and pSTAT1 Alexa 647 (BD Pharmingen) and analyzed with BD FACSCanto according to standard procedures. Data were analyzed with Flowjo software.

Immunohistochemistry and Special Stains

Punch biopsies of lesional skin were fixed in 10% neutral buffered formalin and routinely processed. Serial tissue sections of 5-μm thickness were made and spread on poly-L-lysine coated glass slides. Immunohistochemical staining was carried out using the Ventana Benchmark XT fully automatated slide preparation system (Ventana Medical Systems, Inc) using the following antibodies: MPO (DAKO; 1:1000 dilution), CD163 (Novacastra Laboratories: 1:100 dilution), and KP1/CD68 (DAKO: 1:400 dilution). Staining is developed with 3, 3′-diaminobenzidine tetrahydrochloride and counterstained with Meyer's hematoxylin and mounted. Leder staining (Naphthol AS-D chloracetate esterase or specific esterase), which identifies cells of the granulocyte lineage, from the early promyelocyte stage to mature neutrophils, was carried out using the Sigma-Aldrich 91C-1KT following manufacturer's protocol.

RESULTS

Clinical characteristics in patients with CANDLE

Table 1 summarizes the demographic characteristics and clinical presentation of the affected children. Most patients presented within the first 2–4 weeks of life (all by 6 months of age) with fever and repeated attacks of erythematous and violaceous, annular cutaneous plaques, lasting for a few days or weeks and leaving residual purpura. Later during infancy, patients developed persistent periorbital erythema and edema, finger or toe swelling and hepatomegaly with variable elevation of acute phase reactants. Other common clinical features that developed in the first years of life included progressive loss of peripheral fat (lipodystrophy), failure to thrive, lymphadenopathy and hypochromic or normocytic anemia. More variable findings included perioral swelling, parotitis, conjunctivitis/episcleritis, acanthosis nigricans and hypertrichosis, chondritis, aseptic meningitis, interstitial lung disease, nephritis, epididymitis, hypertriglyceridemia and intermittent positivity of ANA or ANCA autoantibodies (Table 1 and Figure 1). Our series includes 4 previously unreported patients from non-consanguineous families: two Caucasian males and a Hispanic female from the USA (patients 6–8), and one Caucasian male from Spain (patient 9) (Figures 1A–G). An MRI from the thigh showed irregular enhancement of fat, suggesting panniculitis, but no myositis (Figures 1H, I). Synovial enhancement, consistent with joint discomfort and arthralgia and/or arthritis was also seen (Figure 1J).

Responses to treatment have been variable (Table 1). Most clinical symptoms, including cutaneous eruption, joint pain and fever respond to high doses of steroids 1–2mg/kg/day, but rebound with tapering (around 0.5mg/kg/day). Responses to steroid sparing agents have been inconsistent. Methotrexate in combination with calcineurin inhibitors have permitted administration of lower doses of steroids, however skin and joint flares with fever in between led to the further addition of biologics. TNF-alpha inhibitors have provided

temporary improvement in some cases, but flares in others. Anti-IL-1 therapy has not allowed a decrease in steroids, and IL-6 blocking agents have normalized acute phase reactants and anemia, but have had limited success in reducing the cutaneous eruption and improving fatigue (dose ranges of biologics see Table 1). The lipodystrophy has invariably progressed despite immunosuppressive therapy.

Histological evaluation identifies a dense dermal infiltrate of immature neutrophils and activated macrophages

Skin biopsies stained with hematoxyilin and eosin (H&E) were reviewed from all patients. Characteristic features included a dense interstitial infiltrate of mononuclear cells with nuclear atypia and both mature and immature neutrophils, with areas of karyorrhexis (Figure 2A,B). Interstitial dermal collagen degeneration is seen. Immunohistochemical staining disclosed a mononuclear infiltrate composed of immature neutrophils/myeloid precursors (myeloperoxidase and Leder stains, Figure 2C), as well as atypical mononuclear cells that are most likely activated macrophages (positive for CD68-KP1 and CD163, negative for Leder stain) (Figure 2D–F).

Genetic analyses reveal that mutations in *PSMB8* cause CANDLE

A region of homozygosity shared by four patients (patients 1, 2, 4 and 5) was identified in chromosome 6p21 (haplotype cluster rs6924453- rs3763341) (Figure 3A), but not in patient 9. This region spans ~2.7Mb, and includes 164 genes, including 120 protein-coding genes, encompassing the major histocompatibility complex. Given that CANDLE is an immune-mediated disease, with prominent involvement of the skin and adipose tissues, we performed direct sequencing of the following candidate genes: *AGPAT1* (gene ID 10554), *TRIM27* (gene ID 5987), *ITGB1* (gene ID 3688), *SLC39A7* (gene ID 7922), *NOTCH4* (gene ID 4855), *SLC44A4* (gene ID 80736) and *PSMB8* (gene ID 5969).

Sequencing of the six exons of the *PSMB8* gene in patient 5 revealed a homozygous c. 405C>A mutation in exon 3, changing cysteine at amino acid 135 to a stop codon (p.C135X; in accordance with ENST00000374882 transcript) (Figure 3B, supplementary Table 1). The cysteine at position 135 is highly conserved across species. A homozygous missense mutation, c.224C>T, which leads to the substitution of threonine with methionine at position 75 (p.T75M), was found in the patients 1, 2, 4 and 8. Interestingly, two patients were heterozygous for the mutation (patients 7 and 9) and, despite extensive analysis, no second mutation has been found; one patient (patient 6) shows no mutation in *PSMB8*. The genotype of the deceased pt 3 was deduced from her sister (pt 4) as both had the same disease. Mutations for the neighboring subunit *PSMB2*, and the other immunoproteasome (i-proteasome) specific subunits *PSMB9* and *PSMB10* were negative, but further analyses are ongoing (Figure 3C, supplementary Table 1). None of these sequence changes was observed in 750 healthy controls, including 100 Ashkenazi Jews.

Whole exome sequencing done in parallel generated 2.4 Gb of mappable sequence data and achieved 20-fold coverage of the targeted exome. On average, 57.74% of the bases originated from the targeted exome, with 81% of the targeted bases covered at least four times. Initial variant sites calling (>4x) resulted in the identification of 20,012 genetic variants, including 153 within the shared homozygous region on chromosome 6p21. Eight individual reads were mapped back to the genomic position of the c.405C>A *PSMB8* mutation, confirming the homozygous nonsense mutation (Figure 3D).

In silico analysis suggests improper formation of the immunoproteasome

We modeled mutations identified in *PSMB8* in a ribbon diagram (Figure 4A). The β units of the i- proteasome are organized in 2 overlying rings containing 7 subunits each. Two of the

mutations, one previously published in adults with severe lipodystrophy (p.T75M) (10) and the novel nonsense mutation, p.C135X, identified in the Jewish patient are shown (left image). The p.C135X mutation leads to a large deletion of the terminal 141 amino acids of the inducible β5i subunit. Intact residues are shown as red and deleted residues are shown as gray. The deleted residues would normally interact with the neighboring β4 subunit in the same ring, but also bind to the β4 unit of the adjacent ring (right image). The nonsense mutation therefore provided us with structural evidence that the i-proteasome, which requires the incorporation of the β5i subunit, cannot form. The T75 amino acid that is mutated in the other patients is represented by a purple ball.

Functional analyses suggest an inflammatory response involving the interferon pathway

To assess the dysregulated inflammatory response in CANDLE patients, we performed cytokine profiling in serum from peripheral blood of 3 patients: one patient with *PSMB8* mutations on both alleles; one with only one identified *PSMB8* mutation to date; and one without a detectable mutation in *PSMB8*. All showed very high, but variable levels of IP-10. Mean IP-10 levels in CANDLE patients were 77 fold higher than those observed in healthy controls and more than 30 fold higher than in untreated patients with an IL-1 mediated autoinflammatory syndrome neonatal-onset multisystem inflammatory disease (NOMID). Other cytokines that were significantly elevated in CANDLE patients compared to healthy controls and NOMID patients were MCP-1 and RANTES (Figure 4B). Notably, IL-6 and IL-1Ra were modestly elevated not only in CANDLE syndrome patients, but also in patients with NOMID.

The very high levels of IP-10 suggested excessive interferon responses in CANDLE patients (Supplementary figure 1). To probe for evidence of excessive IFN signaling in CANDLE patients in vivo, we assessed the transcriptome in whole blood microarray analysis in four CANDLE patients and four age and gender matched healthy controls. CANDLE patients had 507 genes (650 transcripts) that were more than two-fold differentially expressed compared to healthy controls ($p<0.05$) (Supplementary table 2). Differentially expressed genes (DEGs) were analyzed by the Ingenuity pathway analysis (IPA) program to identify dyregulated canonical pathways and the IFN pathway was the most differentially regulated in CANDLE patients (p=4.73E-06). Of the IFN induced gene list in IPA, most were IFN-γ induced (n=42) and 6 were also regulated by IFNα/β. The genes were plotted on a color-coded heat map and the pattern of increased (shades of red) and decreased DEGs (shades of blue) were strikingly similar among CANDLE patients, regardless of the presence or absence of detectable *PSMB8* mutations (Figure 4C). IP-10 (CXCL10) which is highly expressed in the patients' serum was among the IFN induced upregulated genes. We also compared our DEG list to interferon regulated genes published in www.interferome.org and 119 of the 507 DEGs were found to be interferon regulated.

Since Stat-1 is a downstream mediator of interferon-α/β and -γ signaling, we studied Stat-1 phosphorylation in the monocytes in response to IFN-γ stimulation. Compared with monocytes from healthy controls and a patient with NOMID, monocytes from CANDLE patients showed stronger Stat-1 phosphorylation in response to all IFN-γ concentrations used for stimulation (Figure 5A).

To assess the effect of various treatments the patients received on the IFN induced genes, blood samples from multiple visits were obtained in two patients, including one patient treated at different times with anti-TNF-alpha and anti-IL-6 therapy (supplementary figure 2). Although temporary clinical improvement was seen with anti-TNF-alpha and anti-IL-6 treatment (unpublished observation), the "IFN signature" did not improve. IL-6 blocking therapy normalized IL-6 inducible genes (data not shown) and CRP levels, however, skin

lesions, fatigue or joint pain did not significantly improve and peripheral fat loss progressed, suggesting a possible association between the IFN signature and disease activity.

JAK kinases are critical signaling molecules mediating IFN signaling on the IFN receptors. To determine the effect of a JAK kinase inhibitor, tofacitinib, on the excessive interferon response in CANDLE patients, we assessed its inhibiting effect on stat-1 phosphorylation in patients' monocytes stimulated with IFN-γ. Tofacitinib decreased stat-1 phosphorylation in a dose dependent manner in both CANDLE patients and healthy control monocytes (Figure 5B). Tofacitinib also inhibited IFN-γ induced IP-10 production in PBMC in a dose dependent manner and its inhibitory effect was more efficient than with the IL-1 receptor agonist anakinra or anti-IL-6 blockade with tocilizumab (data not shown). As tofacitinib and other agents blocking the IFN pathways are not available to use as a treatment in our patients, we could not assess the effect of blocking the IFN signaling pathway on the clinical and laboratory symptoms of CANDLE patients.

DISCUSSION

In the current study we identified mutations in the *PSMB8* gene as the cause of CANDLE syndrome, extending the phenotypic spectrum of a novel recently described autoinflammatory syndrome caused by *PSMB8* mutations (10). We also identified dysregulation of the IFN signaling pathway and suggest that the interferon pathway may be a target for treatment in these patients.

After the original report of CANDLE syndrome in four children, a syndrome diagnosed in three adult patients with joint contractures, muscle atrophy, microcytic anemia, and panniculitis-induced childhood-onset lipodystrophy was reported under the acronym "JMP" (10). Patients with JMP were recently demonstrated to carry a mutation in the *PSMB8* gene (8). The patients described were homozygous for the same mutation, p.T75M, that we found in five of our patients (8, 10).

Although CANDLE patients have some overlapping features with JMP patients, including a cutaneous eruption and lipodystrophy (10), none of our patients has developed joint contractures and muscle atrophy was not a prominent disease feature, although two patients (1 and 7) developed an acute, self-healing attack of myositis. CANDLE patients, on the other hand, showed several key features that have not been described in the JMP patients, particularly recurrent febrile episodes, elevated acute phase reactants and a characteristic neutrophilic dermatosis with a mononuclear interstitial infiltrate including "immature" neutrophils in the dermis that seems pathognomonic for CANDLE syndrome. In fact two patients have been misdiagnosed as acute cutaneous myelogenous leukemia. Nevertheless, the detection of the same and additional mutations in *PSMB8* unifies these disorders as a novel i-proteasome associated autoinflammatory syndrome. Clinical reports of children with disease manifestations that closely resemble CANDLE syndrome from families in Japan and Lebanon (11–13) might allow for the discovery of further molecular causes of this disease. While our data in young children illustrate manifestations of early severe, and potentially lethal disease and alert to the fact that muscle involvement and joint contractures may not present until later in life, the findings in the adult patients likely illustrate the natural course of the disease in untreated or partially treated patients (10, 11).

In one of our patients, no mutation in *PSMB8* was discovered, and two patients showed a mutation in only 1 allele, despite sequencing the entire exonic and intronic sequence of the gene. In the boy without a mutation on either allele (patient 6), we similarly found no mutation in sequencing the two other i-proteasome specific subunits. These data indicate

genetic heterogeneity underlying CANDLE syndrome and raises the prospect of other genes as the genetic cause for CANDLE syndrome.

The gene mutated in CANDLE, *PSMB8*, encodes the inducible β5i subunit of the proteasome, a protein complexe that consists of two α rings and two β rings, each ring is formed of 7 different globular α or β-subunits. Proteasomes are evolutionary conserved cylindrical structures that are critical for protein degradation (14). Upon IFN stimulation critical subunits of a constitutive proteasome, the β1, 2 and 5 subunits, are replaced with inducible i-subunits, β1i, β2i and β5i, to form i-proteasomes which are highly expressed in hemopoietic cells (15).

The functions of the i-proteasomes have been studied *in vitro* and in animal models. The i-proteasome can generate antigenic peptides for MHC class I presentation (16), but recent data in *psmb8/lmp7* knockout mice (17) suggest an important additional role in maintaining cell homeostasis by removing accumulating proteins marked for degradation from the cells (18). Cellular stress such as infections or radiation lead to type I IFN induced production of reactive oxygen species and newly synthesized proteins that are particularly sensitive to oxidation (19–21). Failure to process/degrade protein will result in formation of ubiquitin-rich cytoplasmic aggregates or inclusions and consequently increase cellular sensitivity to apoptosis (18). It is thought that the excessive demand for protein processing/degradation is mainly met by cytokine-mediated upregulation of the ubiquitination machinery and increased assembly of the highly efficient i-proteasome (22, 23).

The persistent IFN signature in CANDLE patients on microarray and the increased Stat-1 phosphorylation in monocytes from CANDLE patients in response to IFN-γ stimulation could reflect ongoing “cellular stress” in CANDLE patients. In concordance with the current understanding of the i-proteasome function, we have suggested a disease model (supplementary figure 1) which proposes that defects in i-proteasome function may lead to accumulation of damaged proteins resulting in more cellular stress and a vicious cycle of increased IFN signaling. Interestingly, CANDLE flares are observed with infections and other stressful events. Some cells such as fat or muscle cells may be subject to cellular apoptosis due to accumulation of damaged proteins. In fact a Japanese patient with severe fat loss, muscle atrophy and suspected CANDLE syndrome died of cardiac failure at the age of 47. Histological examination of skeletal muscle on autopsy revealed intramitochondrial paracrystalline inclusions and cytoplasmic and myeloid bodies in muscle cells (24). Whether the inclusions seen constitute accumulation of oxidant damaged/aggregated proteins that cause cell death is an attractive hypothesis to account for muscle loss later in life, but studies on the cell specific effect of the i-proteasome deficiency are needed to explain the observed visceral effects of the mutations.

IP-10 is a type I or type II IFN induced protein, that functions as a C-X-C motif chemokine, also known as CXCL10 (supplementary figure 1). It is produced in a variety of cell types, including endothelial cells, keratinocytes, fibroblasts, mesangial cells, monocytes, dendritic cells, neutrophils and activated T cells (25). IP-10/CXCL10 is an important chemoattractant for effector T cells, its serum level has been shown to correlate with the extent of T cell infiltration in the tissue. IP-10 may contribute to the pathology in CANDLE patients by acting as a chemoattractant for T cells into tissues such as the skin with the described inflammatory infiltrate. Whether the inflammatory skin infiltrate of immature neutrophils and activated myeloperoxidase positive histiocytic cells is a consequence of IFN signaling needs further evaluation. However, the important role of IFN-γ in the recruitment of neutrophils through the induction of CCL3 (26) and the stimulation of myeloperoxidase production in monocyte/macrophages (27) are consistent with a possible pathogenic role of IFN in skin.

Given our own data and the clinical reports of devastating disease manifestations in adults, the outcome of untreated disease is expected to be poor. The partial responses and the continued need for steroids despite being on treatment with targeted therapies including IL-1 receptor antagonist, TNF-alpha blockage and IL-6 receptor inhibitors (see Table 1) urge the need for a better understanding of the disease pathogenesis and for identifying more effective targets for therapeutic intervention. Whether the persistence of the IFN signature on the treatment with targeted agents offers a clue to a more effective intervention is a testable hypothesis as agents blocking IFN signaling (including JAK inhibitors) are in clinical trials.

CANDLE and the other *PSMB8*-associated syndromes illustrate the profound effect of i-proteasome dysfunction on inflammation and organ function. In the current study we have established *PSMB8* as the causative gene for CANDLE syndrome and describe clinical and histological features that can establish early diagnosis. The mutations in *PSMB8*, also found in JMP, illustrate the clinical and genetic spectrum of this novel i-proteasome associated autoinflammatory syndrome. Further studies to fully explore the role of the i-proteasome in autoinflammatory diseases and to identify other mutations in PSMB8 mutation negative CANDLE patients are needed and are ongoing.

Supplementary Material

Refer to Web version on PubMed Central for supplementary material.

Acknowledgments

This research was supported by the Intramural Research Program of the National Institute of Arthritis and Musculoskeletal and Skin Diseases at the NIH, and by the Authority for Research and Development, Hebrew University of Jerusalem (AZ), the Hadassah Medical Center Young Clinician Award (YR).

The authors would like to thank Nikki Plass, RN., Deborah Stone M.D., Dawn Chapelle RN, Sapna Patel Vaghani, MD, and Rhina Castillo MD, for their help organizing patient visits and patient examinations. Adam Reinhardt MD, Elizabeth Brown MD, Paulina Navon-Elkan MD and Kristina Rother MD for their collaboration on patient treatment, Ivona Aksentijevich MD for her help with the interpretation of the genetic data, Hang Pham, MT for her help with the cytokine analysis, Max Gadina, PhD for his help with the initial cytokine analysis and the sharing of the synthetic CP-690550 (tofacitinib), and Isabel Colmenero MD, Luis Requena MD and Heinz Kutzner MD for their help in immunohistochemistry studies.

References

1. Masters SL, Simon A, Aksentijevich I, Kastner DL. Horror autoinflammaticus: the molecular pathophysiology of autoinflammatory disease (*). Annu Rev Immunol. 2009; 27:621–68. [PubMed: 19302049]
2. Henderson C, Goldbach-Mansky R. Monogenic autoinflammatory diseases: new insights into clinical aspects and pathogenesis. Curr Opin Rheumatol. 22:567–78. [PubMed: 20671522]
3. McGonagle D, McDermott MF. A proposed classification of the immunological diseases. PLoS Med. 2006; 3:e297. [PubMed: 16942393]
4. Goldbach-Mansky R. Blocking interleukin-1 in rheumatic diseases. Ann N Y Acad Sci. 2009; 1182:111–23. [PubMed: 20074280]
5. Torrelo A, Patel S, Colmenero I, Gurbindo D, Lendinez F, Hernandez A, et al. Chronic atypical neutrophilic dermatosis with lipodystrophy and elevated temperature (CANDLE) syndrome. J Am Acad Dermatol. 62:489–95. [PubMed: 20159315]
6. Ramot Y, Czarnowicki T, Maly A, Navon-Elkan P, Zlotogorski A. Chronic Atypical Neutrophilic Dermatosis with Lipodystrophy and Elevated Temperature Syndrome: A Case Report. Pediatr Dermatol. 2010 Jun 9. [Epud ahead of print].
7. Seelow D, Schuelke M, Hildebrandt F, Nurnberg P. HomozygosityMapper--an interactive approach to homozygosity mapping. Nucleic Acids Res. 2009; 37:W593–9. [PubMed: 19465395]

8. Agarwal AK, Xing C, DeMartino GN, Mizrachi D, Hernandez MD, Sousa AB, et al. PSMB8 encoding the beta5i proteasome subunit is mutated in joint contractures, muscle atrophy, microcytic anemia, and panniculitis-induced lipodystrophy syndrome. Am J Hum Genet. 87:866–72. [PubMed: 21129723]
9. Unno M, Mizushima T, Morimoto Y, Tomisugi Y, Tanaka K, Yasuoka N, et al. The structure of the mammalian 20S proteasome at 2.75 A resolution. Structure. 2002; 10:609–18. [PubMed: 12015144]
10. Garg A, Hernandez MD, Sousa AB, Subramanyam L, Martinez de Villarreal L, dos Santos HG, et al. An autosomal recessive syndrome of joint contractures, muscular atrophy, microcytic anemia, and panniculitis-associated lipodystrophy. J Clin Endocrinol Metab. 95:E58–63. [PubMed: 20534754]
11. Kitano Y, Matsunaga E, Morimoto T, Okada N, Sano S. A syndrome with nodular erythema, elongated and thickened fingers, and emaciation. Arch Dermatol. 1985; 121:1053–6. [PubMed: 4026345]
12. Megarbane A, Sanders A, Chouery E, Delague V, Medlej-Hashim M, Torbey PH. An unknown autoinflammatory syndrome associated with short stature and dysmorphic features in a young boy. J Rheumatol. 2002; 29:1084–7. [PubMed: 12022327]
13. Tanaka M, Miyatani N, Yamada S, Miyashita K, Toyoshima I, Sakuma K, et al. Hereditary lipo-muscular atrophy with joint contracture, skin eruptions and hyper-gamma-globulinemia: a new syndrome. Intern Med. 1993; 32:42–5. [PubMed: 8495043]
14. Jung T, Catalgol B, Grune T. The proteasomal system. Mol Aspects Med. 2009; 30:191–296. [PubMed: 19371762]
15. Rivett AJ, Hearn AR. Proteasome function in antigen presentation: immunoproteasome complexes, Peptide production, and interactions with viral proteins. Curr Protein Pept Sci. 2004; 5:153–61. [PubMed: 15180520]
16. Yewdell JW. The seven dirty little secrets of major histocompatibility complex class I antigen processing. Immunol Rev. 2005; 207:8–18. [PubMed: 16181323]
17. Moebius J, van den Broek M, Groettrup M, Basler M. Immunoproteasomes are essential for survival and expansion of T cells in virus-infected mice. Eur J Immunol. 2010; 40:3439–49. [PubMed: 21108466]
18. Seifert U, Bialy LP, Ebstein F, Bech-Otschir D, Voigt A, Schroter F, et al. Immunoproteasomes preserve protein homeostasis upon interferon-induced oxidative stress. Cell. 2010; 142:613–24. [PubMed: 20723761]
19. Lelouard H, Schmidt EK, Camosseto V, Clavarino G, Ceppi M, Hsu HT, et al. Regulation of translation is required for dendritic cell function and survival during activation. J Cell Biol. 2007; 179:1427–39. [PubMed: 18166652]
20. Medicherla B, Goldberg AL. Heat shock and oxygen radicals stimulate ubiquitin-dependent degradation mainly of newly synthesized proteins. J Cell Biol. 2008; 182:663–73. [PubMed: 18725537]
21. Reits EA, Hodge JW, Herberts CA, Groothuis TA, Chakraborty M, Wansley EK, et al. Radiation modulates the peptide repertoire, enhances MHC class I expression, and induces successful antitumor immunotherapy. J Exp Med. 2006; 203:1259–71. [PubMed: 16636135]
22. Strehl B, Textoris-Taube K, Jakel S, Voigt A, Henklein P, Steinhoff U, et al. Antitopes define preferential proteasomal cleavage site usage. J Biol Chem. 2008; 283:17891–7. [PubMed: 18424434]
23. Voigt A, Jakel S, Textoris-Taube K, Keller C, Drung I, Szalay G, et al. Generation of in silico predicted coxsackievirus B3-derived MHC class I epitopes by proteasomes. Amino Acids. 2010; 39:243–55. [PubMed: 19997756]
24. Oyanagi K, Sasaki K, Ohama E, Ikuta F, Kawakami A, Miyatani N, et al. An autopsy case of a syndrome with muscular atrophy, decreased subcutaneous fat, skin eruption and hyper gamma-globulinemia: peculiar vascular changes and muscle fiber degeneration. Acta Neuropathol. 1987; 73:313–9. [PubMed: 3618123]
25. Lee EY, Lee ZH, Song YW. CXCL10 and autoimmune diseases. Autoimmun Rev. 2009; 8:379–83. [PubMed: 19105984]

26. Bonville CA, Percopo CM, Dyer KD, Gao J, Prussin C, Foster B, et al. Interferon-gamma coordinates CCL3-mediated neutrophil recruitment in vivo. BMC Immunol. 2009; 10:14. [PubMed: 19298652]

27. Chase MJ, Klebanoff SJ. Viricidal effect of stimulated human mononuclear phagocytes on human immunodeficiency virus type 1. Proc Natl Acad Sci USA. 1992; 89:5582–5. [PubMed: 1319066]

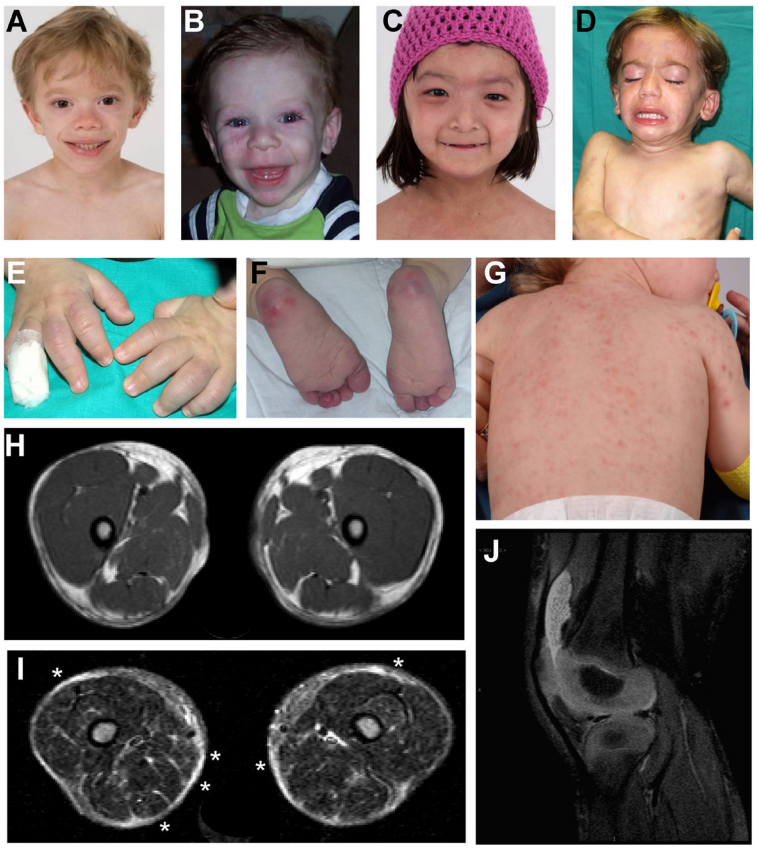

Figure 1.

Clinical features of CANDLE syndrome. **A–D:** Facial features and eruption in patients with CANDLE. Note the violaceous periorbital discoloration and edema, perinasal erythema, and significant fat loss most prominent in B. **E, F:** Finger swelling and violaceous lesions on the heel and toes. **G:** Discrete erythematous nodules and post-inflammatory hyperpigmentation. **H, I:** T2-weighted MRI of thighs (H) in one patient suggested loss of subcutaneous fat, particularly on the posterior aspect of both thighs; STIR image (I) showed increased signal intensity in the subcutaneous fat, suggesting panniculitis (asterisks). **J:** Synovial enhancement with rice body formation extending to the suprapatellar pouch.

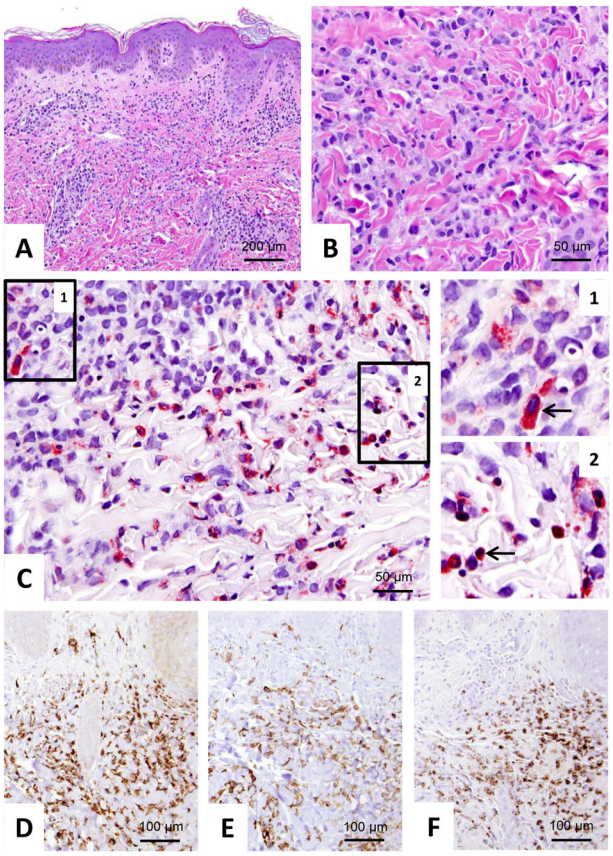

Figure 2.

Histopathology of lesional skin. **A:** H&E staining showed a dense perivascular and interstitial mononuclear dermal infiltrate. The overlying epidermis appears unremarkable. (H&E, 100× original magnification). **B:** Areas of karyorrhexis are shown. (H&E, 400× original magnification); **C:** Leder stain (Naphthol AS-D chloracetate esterase stain or specific esterase) specifically identifies cells of the granulocyte lineage, from the early promyelocyte stage to mature neutrophils. At high magnification (C-1: right upper panel), some of the mononuclear cells are Leder stain-positive, suggestive of immature neutrophils, and rare mature neutrophils. Another high magnification view (C-2: right lower panel) also shows karyorrhectic nuclear debris surrounded by a rim of Leder stain positive cytoplasm. (Leder stain, 400× original magnification). **D–F:** Staining for the macrophage markers KP-1 (CD68) (D) and CD163 (E), and myeloperoxidase positive cells (F). (Immunohistochemical stains, 200× original magnification).

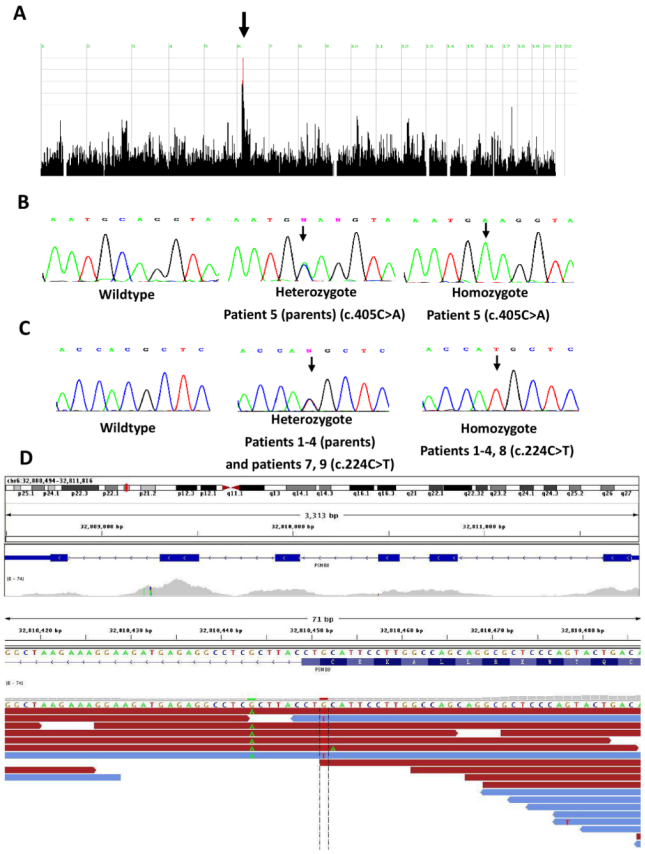

Figure 3.

Genetic analyses. **A:** Genome-wide homozygosity peaks discovered by HomozygosityMapper analysis. Black arrow indicates the chromosomal region of homozygosity shared by four patients (patients 1, 2, 4 and 5). **B:** Sequence analysis of *PSMB8*. a) wild type; b) heterozygous c.405C>A mutation; and c) homozygous c.405C>A mutation in patient 5. **C:** Sequence analysis of *PSMB8*. a) wild type; b) heterozygous c. 224C>T mutation; and c) homozygous c.224C>T mutation in patients 1, 2, 4, 7, 8 and 9. **D:** Overview of *PSMB8* coverage by exome sequencing demonstrating the identification of a homozygous mutation in *PSMB8*.

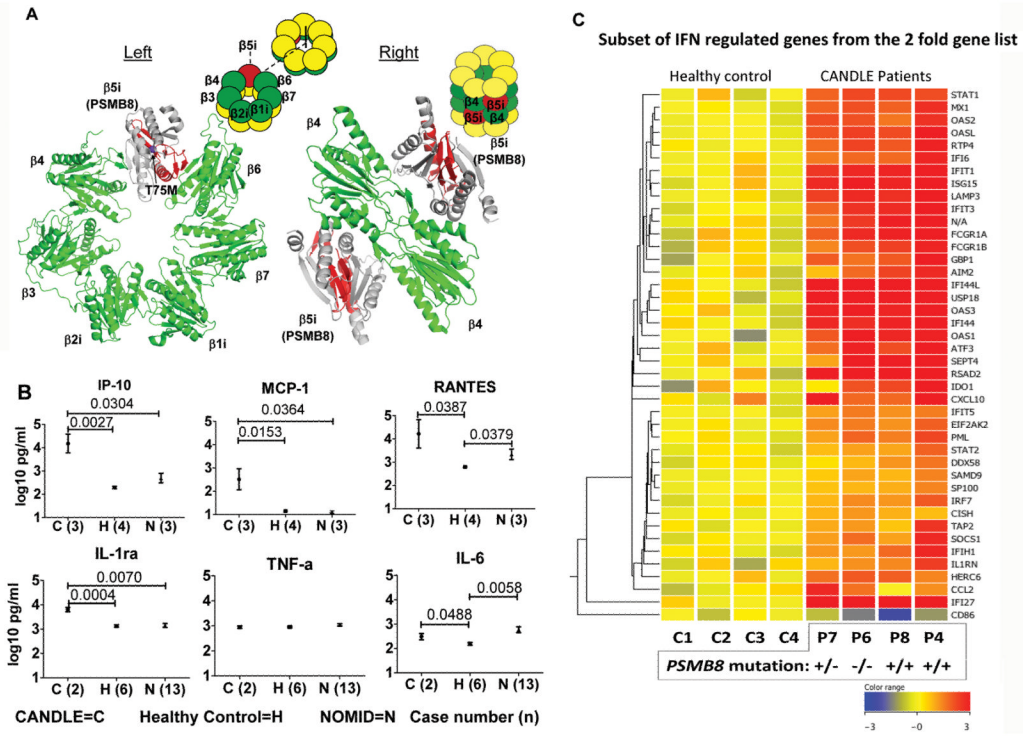

Figure 4.

Functional assessment of *PSMB8* mutations. **A:** Structural model of 20S proteasome. The model on the left shows a ring of β subunits in a proteasome, the inset on the upper right corner shows the position of the ring in 20S proteasome. The intact residues of the β5i subunit in the patient with the C135X mutation are shown in red and the deleted residues in gray. The T75 amino acid is represented by a purple ball. The model on the right shows two β4 subunits interacting with two β5i subunits on two adjacent rings, the inset on the upper right corner shows their position in a 20S proteasome. **B:** Cytokine expression in CANDLE patients 6, 7, 8, healthy controls, and NOMID patients. Data are shown on a log10 scale with error bars indicating standard errors of the mean (SEM). **C:** Whole blood microarray analysis was done on 4 CANDLE patients and 4 healthy age/gender matched controls. A color-coded heat map was generated on 42 IFN regulated genes from a transcript list that were two fold differentially expressed ($p<0.05$). Red indicates increased expression levels and blue indicates decreased expression levels compared to the mean of healthy controls.

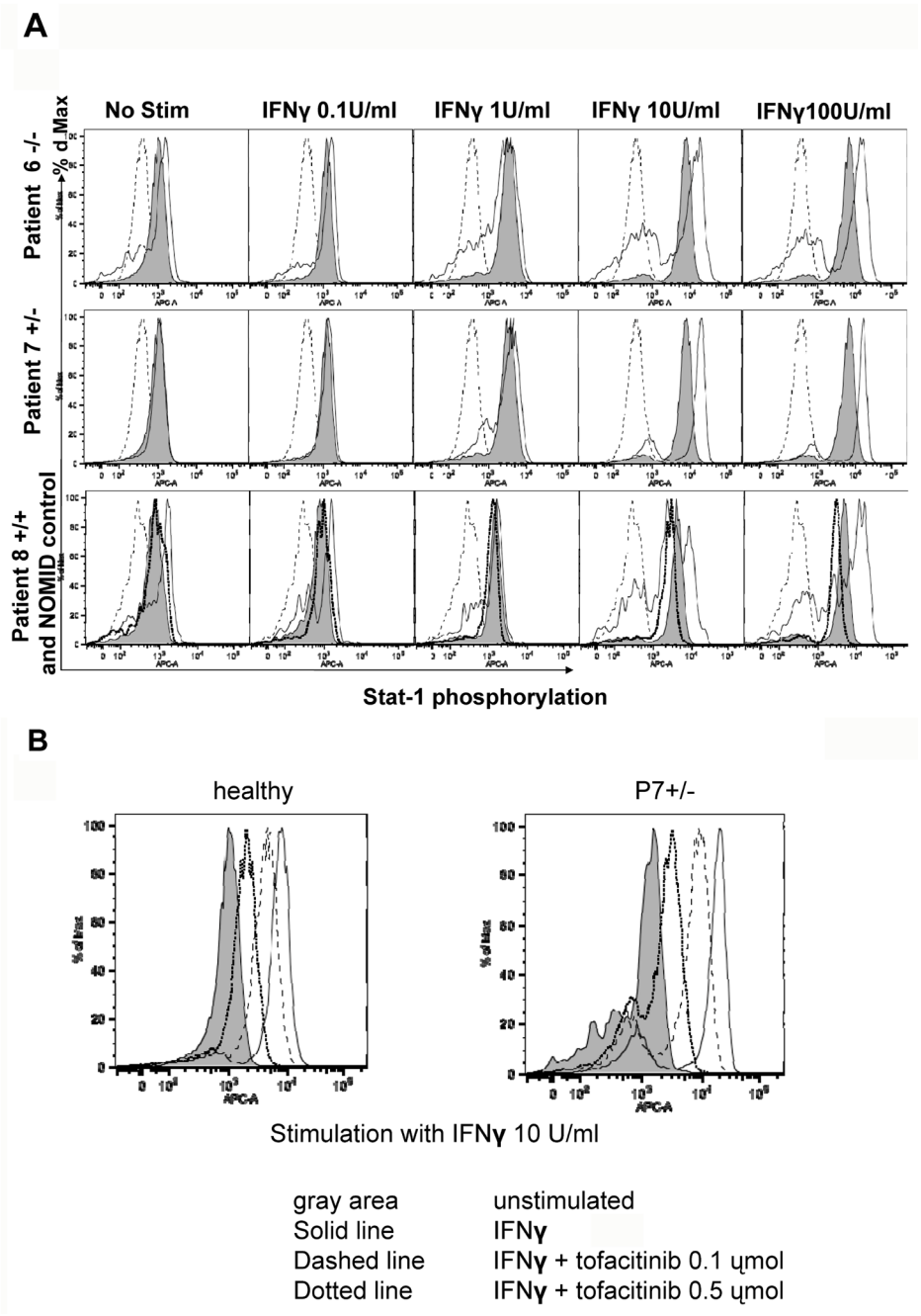

Figure 5.

Stat-1 -phosphorylation in CANDLE patients' monocytes in response to IFN-γ stimulation, and inhibition by a JAK kinase inhibitor (tofacitinib). **A:** Stat-1 phosphorylation in response to 15 min IFN-γ stimulation in monocytes from CANDLE patients, healthy controls and a NOMID patient. The dashed line indicates an isotype control, the solid gray graph indicates the response of a healthy control and the solid line of the CANDLE patient. In the lower panels the bolded dashed line indicates the response of a NOMID patient. **B**: PBMCs from a healthy control and from pt7 were stimulated with 10IU/ml IFN-γ for 15 min in the absence (solid line) and presence of in 0.1 and 0.5μmol of tofacitinib (dashed and dotted lines

respectively). A dose depended inhibition in stat-1 phosphorylation is seen in patient and control.

Arthritis Rheum. Author manuscript; available in PMC 2013 March 1.

Table 1

Demographics and Clinical Disease Manifestations

Demographic Characteristics	Patient 1*	Patient 2*	Patient 3*	Patient 4*	Patient 5*	Patient 6	Patient 7	Patient 8	Patient 9
Age yr	13	10	Died at 14yrs	2	12.5	5.5	3.5	6	2.5
Sex	Male	Female	Female	Female	Male	Male	Male	Female	Male
Ethnicity/Origin	Spanish	Spanish	Hispanic	Hispanic	Jewish-Ashkenazi	Americ/Caucasian	Amerc/Caucasian	Hispanic	Spanish
Clinical Outcome	Alive and Failure to thrive	Alive and Failure to thrive	Deceased age 14 years	Alive and Failure to thrive	Alive and Failure to thrive	Alive and Failure to thrive	Alive	Alive	Alive
Clinical Characteristics									
Age of clinical presentation	1 month	6 months	During 1st 6 months	1 week	1 month	2weeks	2 months	2 weeks	1 month
Symptoms of initial presentation	Fever and skin lesions	Fever and skin lesions	Fever, violaceous plaques and nodules and hepatomegaly	Violaceous annular plaques	Fever and skin lesions	Rash and foot swelling, periorbital erythema	Periorbital erythema and swelling	Fever, violaceous plaques periorbital and erythema	Fever and skin lesions
Recurrent fevers and elevated acute phase reactants (ESR, CRP)	+	+	+	+	+	+	+	+	+
Annular plaques	+	+	+	+	+	+	+	+	+
Lipodystrophy	Yes/peripheral, especially face and upper limbs	Yes/upper limbs and cheeks	Yes/peripheral and face	Yes	Yes	Yes/upper and lower body	Yes/upper body mainly proximal	yes/upper body	+
Finger swelling	+	+	+	+	+	+	–	–	+
Hepatosplenomegaly	+	+ (only hepatomegaly)	+ (only hepatomegaly)	+ (only hepatomegaly)	+ (only hepatomegaly)	+	+	Upper limit of normal	–
Lymphadenopathy	+	+	–	+	–	+	+	+	+
Low weight and height	+	+	+	+	+	+	–	–	
Muscle atrophy	+	+	–	+	–	–	–	–	+
Arthritis/arthralgia	+	+	+	+	+	+	+	+	+
Prominent abdomen	+	+/–	+	+	+	+	–	–	+
Violaceous eyelids	+	+	+	+	+	+	+	+	+
Anemia and other hematologic manifestations	Hypochromic anemia and increased platelet counts	Hypochromic anemia	Hypochromic anemia	Hypochromic anemia and increased platelet counts	Hypochromic anemia	Hypochromic anemia	Neutropenia and thrombocytopenia	Hypochromic anemia in the past	Hypochromic anemia
Elevated LFTs	+	+	+	+	+	intermittent	+	–	+
MORE VARIABLE FINDINGS									
Perioral swelling	+	+	–	+	+	–	–	–	+
Parotitis	–	–	+	+	–	–	–	–	–
Conjunctivitis/episcleritis	+	+	–	+	–	–	–	–	+
Acanthosis nigricans	–	–	+	+	–	–	+	–	–
Hypertrichosis	–	–	+	+	+	–	+	+	–
Ear and nose chondritis	+	Slight nose chondritis	–	–	–	–	–	possible	+
Wide-spaced nipples	+	+	–	–	+	–	–	–	+
Aseptic meningitis	+	–	+	–	–	–	–	–	–
Basal ganglia calcifications	+	–	+	–	–	ND§	ND	ND	–

Demographic Characteristics	Patient 1*	Patient 2*	Patient 3*	Patient 4*	Patient 5*	Patient 6	Patient 7	Patient 8	Patient 9
Lung manifestations	–	–	Interstitial lung disease	–	–	BOOP like	–	–	–
Nephritis	–	–	+	–	–	–	–	–	–
Recurrent infections	–	–	Otitis	Otitis	–	Otitis and recurrent sinusitis	Otitis and recurrent sinusitis	Recurrent upper respiratory infections	+
Epididymitis	+	NA†	NA	NA	–	–	+	NA	–
Metabolic manifestations	–	–	Hyper- triglyceridemia	Hyper- triglyceridemia	Elevated TSH Triglycerides ND	Mild hyper- triglyceridemia		Elevated TSH, high LDL and triglycerides	Low HDL
Autoantibodies (intermittent)	–	–	Coombs-positive hemolytic anemia Positive lupus anticoagulant	–	Alopecia areata and positive C-ANCA	–	ANCA 1:20 now negative	ANA antibody positive in past	Hypergammaglobuli nemia
Treatments	NSAIDs Colchicine Dapsone Methotrexate Etanercept Anakinra	NSAIDs PUVA Methotrexate	NSAIDs Methotrexate Azathioprine Infliximab Cyclosporine Rituximab Pulsed steroids	IVIG Anakinra Dapsone Ibuprofen Pulsed steroids	Hydroxychloroquine Pulsed steroids	Tacrolimus** Methotrexate** Prednisolone†† Infliximab** Methylprednisolone Adalimumab** Anakinra** Tocilizumab**	Tacrolimus** Methotrexate** Prednisolone†† Tocilizumab** Methylprednisolone	Prednisone†† Methylprednisolone Anakinra** Adalimumab** Tocilizumab**	No

*Patients were previously reported

†NA denotes: not applicable

§ND demotes not done

**Drug doses and treatment duration in these patients were known and dose ranges and maximal exposure times were as follows (methotrexate (for greater than 4 years), tacrolimus (4mg/day for greater than 12 months), infliximab (5– 12.5mg/kg/dose q 4 weeks up to 12 months), adalimumab (20–40mg q10 days for 4 months then discontinued), anakinra (1–5mg/kg/day for 3 months), tocilizumab (5–12mg/kg/dose q14 days, 2 patients are still on treatment >6 months, one developed a drug reaction warranting discontinuation), pts 5 and 6 were on prednisolone and tacrolimus in addition to one biologic, pt 7 is on prednisone in combination with tocilizumab.

††Prednisone is tapered to control symptoms of fever, rash and joint pain with doses between 0.3–3mg/kg/dose and pulses have been administered in between to control symptoms